Product Channels of the HCCO + NO Reaction†

Justin P. Meyer and John F. Hershberger*

Department of Chemistry and Molecular Biology, North Dakota State University, Fargo, North Dakota 58105

Received: July 22, 2004; In Final Form: November 20, 2005

The product branching ratio of the HCCO + NO reaction was investigated using the laser photolysis/infrared absorption technique. Ethyl ethynyl ether (C_2H_5OCCH) was used as the HCCO radical precursor. Transient infrared detection of CO, CO_2, and HCNO products was used to determine the following branching ratios at 296 K: $\phi(CO+HCNO) = 0.78 \pm 0.04$ and $\phi(CO_2+HCN) = 0.22 \pm 0.04$. These values are in good agreement with some recent ab initio calculations.

Introduction

The spectroscopy[1−4] and kinetics[4−9] of the ketenyl radical (HCCO) is of interest, partly because of the role this species plays in combustion chemistry. HCCO is formed in flames primarily by the oxidation of acetylene.[10,11] It has been observed in laboratory studies by infrared absorption[4] and laser-induced fluorescence spectroscopy.[1,2] Several kinetic studies involving HCCO have appeared recently, with total rate constant measurements reported for reactions with NO,[4−7,9] NO_2,[5] O_2,[5] O,[8] and C_2H_2.[5] The reaction with NO is of particular interest because of the role it plays in NO-reburning mechanisms[12−17] for the reduction of NO_x emissions from fossil-fuel combustion processes. Several product channels are possible:

$$\mathrm{HCCO + NO \rightarrow CO_2 + (HCN)} \qquad \Delta H^0 = -527.2 \text{ kJ/mol} \tag{1a}$$

$$\rightarrow \mathrm{CO + (HCNO)} \qquad \Delta H^0 = -200.8 \text{ kJ/mol} \tag{1b}$$

$$\rightarrow \mathrm{NCO + HCO} \qquad \Delta H^0 = -71.1 \text{ kJ/mol} \tag{1c}$$

The thermochemistry shown is for HCN and HCNO, but several other isomers of these species represent possible, albeit unlikely product channels as well. Several reports of the total rate constant of this reaction have appeared. Unfried et al. used infrared absorption near 2023 cm^{-1} to detect HCCO, and reported $k_1 = (3.9 \pm 0.5) \times 10^{-11}$ cm^3 $molecule^{-1}$ s^{-1} at 298 K.[4] Temps et al. used far-infrared laser magnetic resonance to detect HCCO and obtained $(2.2 \pm 0.6) \times 10^{-11}$ cm^3 $molecule^{-1}$ s^{-1} at 298 K.[5] Boullart et al. used discharge flow-mass spectrometry to obtain $k_1 = (1.0 \pm 0.3) \times 10^{-10} \exp[-350 \pm 150)/T]$ cm^3 $molecule^{-1}$ s^{-1} over the temperature range 290−670 K.[6] In the most extensive kinetic study reported to date, Carl et al. used a laser-induced fluorescence technique to obtain $k_1 = (1.6 \pm 0.2) \times 10^{-11} \exp(340 \pm 30 \text{ K/T})$ cm^3 s^{-1} $molecule^{-1}$ over the temperature range 297−802 K.[9]

Several previous studies have also investigated the product branching in this reaction. In an early prediction, Miller et al. used statistical theories and a QCISD potential surface of Nguyen et al.[7] to predict that CO_2+HCN as the major channel ($\phi_{1a} = 0.81$) at 300 K with a moderate temperature dependence, decreasing to about 0.32 at 2000 K.[13] Kinetic modeling of flow reactor experiments at 1100−1400 K were originally best fit by a branching ratio of $\phi_{1a} = 0.65$,[14] but subsequent calculations on the OH+HCNO reaction suggested that a lower value of ϕ_{1a} may better fit the model.[17] Other more direct experiments as well as subsequent ab initio calculations have contradicted the early results, showing that channel (1a) is in fact the minor channel. Boullart et al., in their mass spectrometry study, reported the following product branching ratios at 700 K: $\phi_{1a} = 0.23 \pm 0.09$, $\phi_{1b} = 0.77 \pm 0.09$.[6] Eickhoff and Temps obtained similar results at 300 K ($\phi_{1a} = 0.28 \pm 0.10$, $\phi_b = 0.64 \pm 0.12$) in an FTIR study.[18] An infrared laser study in our laboratory yielded an even lower branching ratio of $\phi_{1a} = 0.12 \pm 0.04$.[19] Two recent computational studies have improved on the earlier potential energy surface, predicting $\phi_{1a} = 0.22$ at 300 K[20] and $\phi_{1a} = 0.27$ at 300 K.[21] The primary difference between the recent and earlier calculations is that the recent calculations more correctly describe the isomerization barrier between *cis*- and *trans*-OCC(H)NO minima,[20,21] which the earlier calculation had assumed to be a low barrier free rotation.[7] Although either isomer can form HCNO + CO by carbon−carbon bond fission, only the cis isomer can rearrange into a four-membered ring intermediate which decomposes to HCN + CO_2. This barrier therefore represents an important bottleneck in the formation of products (1a). Both of the recent calculations predict a very gradual decrease in ϕ_{1a} with increasing *T*, to ∼0.1 at ∼2500 K.

All the previous experimental studies of this reaction have been complicated by the lack of an ideal precursor for generation of the HCCO radical. Several of the experiments used the O + C_2H_2 reaction to form HCCO + H. This reaction is quite slow, and also produces CH_2 + CO products, requiring the data be fit to a substantial kinetic model. Our previous report[19] used ketene (CH_2CO) as a photolytic precursor at 193 nm. This has the similar problem that CH_2 + CO are the major photolysis products, and H + HCCO is only a minor channel.[22] As a result, any attempt to detect the HCNO product suffers from secondary chemistry, primarily CH_2 + NO → H + HCNO.[23]

In the experiments reported here, we use ethyl ethynyl ether, C_2H_5OCCH, as a photolytic precursor. The 193 nm photodissociation dynamics of this molecule has been recently studied,[24] and this molecule was found to be a relatively clean source of HCCO (and C_2H_5) radicals. Since the ethyl radical does not react quickly with NO, this represents a nearly ideal source of

† Part of the special issue "George W. Flynn Festschrift".

10.1021/jp040503h CCC: $30.25
Published on Web 02/18/2005

HCCO for our experiments. This molecule has been used in one previous kinetic study, a recent report on the HCCO + O_2 reaction.[25]

Experimental Section

The experimental procedure is similar to that described in previous publications.[26,27] 193 nm photolysis light was provided by an excimer laser (Lambda Physik, Compex 200). Several lead salt diode lasers (Laser Components) operating in the 80−110 K temperature range were used to provide tunable infrared probe laser light. The IR beam was collimated by a lens and combined with the UV light by means of a dichroic mirror, and both beams were copropagated through a 1.46 m absorption cell. After the UV light was removed by a second dichroic mirror, the infrared beam was then passed into a 1/4m monochromator and focused onto a 1 mm InSb detector (Cincinnati Electronics, ~1 μs response time). Transient infrared absorption signals were recorded on a LeCroy 9310A digital oscilloscope and transferred to a computer for analysis.

SF_6, Xe, and CF_4 (Matheson) were purified by repeated freeze−pump−thaw cycles at 77K. Traces of CO_2 was removed from SF_6 by the use of an Ascarite trap. NO (Matheson) was purified by repeated freeze−pump−thaw cycles at 163 K to remove NO_2 and N_2O. C_2H_5OCCH in hexane samples were obtained from Aldrich and were purified by several freeze−pump−thaw cycles followed by pumping away of most of the hexane. Small quantities of hexane in the reaction mixtures are not expected to affect the results.

Authentic samples of HCNO for calibration purposes were synthesized by vacuum pyrolysis of 3-phenyl-4-oximinoisoxazol-5-(4*H*)-one as described in the literature,[28,29] and purified by vacuum distillation to remove CO_2 and phenyl cyanide byproducts as well as HNCO impurities. Care was taken to minimize exposure of HCNO to metal to minimize decomposition. In general, HCNO could be allowed to stand at room temperature for ~5 min in our Pyrex absorption cell with minimal decomposition, but ~50% decomposition over 5 min was commonly observed if the sample was in contact with stainless steel vacuum lines.

CO, N_2O, CO_2, and HCNO product molecules were probed using the following absorption lines:

CO ($v = 1 \leftarrow v = 0$)	P(9), P(10), P(16) at 2107.424, 2103.270, 2203.161 cm^{-1}
N_2O (00°1) ← (00°0)	P(32) at 2193.540 cm^{-1}
CO_2 (00°1) ← (00°0)	P(18), P(14) at 2334.157, 2337.659 cm^{-1}
HCNO (0100°0°) ← (0000°0°)	R(10) at 2203.851 cm^{-1}

The HITRAN molecular database was used to locate and identify the spectral lines of CO, N_2O, and CO_2 product molecules.[30] Other published spectral data[31] were used to locate and identify HCNO lines. The spectral lines used are near the peak of the rotational Boltzmann distribution, minimizing sensitivity to small heating effects. For CO_2 product molecule measurements, the infrared laser beam path was purged with N_2 to remove atmospheric CO_2.

Typical experimental conditions were $P_{C_2H_5OCCH} = 0.01-0.02$ Torr, $P_{SF_6} = 0.5$ Torr, and $P_{NO} = 0-0.6$ Torr.

Results and Discussion

Time-resolved transient absorption signals of product molecules at 296 K are shown in Figure 1. The CO_2 and HCNO transient signals displayed rapid rise times followed by slow decays. The CO signals have both a fast and a moderately slow (~150 μs) rise. All of these rise times are slower than would be predicted by the rate constant for reaction 1. This is presumably due to the formation of excited vibrational states of the various product molecules. Since we probe infrared transitions originating from the vibrational ground state, the observed rise time is essentially a measure of the rate of vibrational relaxation of this excited nascent distribution. Previous experiments in our laboratory[26,32] as well as vibrational energy transfer measurements[33−36] have demonstrated that SF_6 is an efficient buffer gas for the relaxation of vibrationally excited CO_2 or N_2O to a Boltzmann distribution, but that CF_4 is a more efficient relaxer of vibrationally excited CO. As a result, SF_6 buffer gas was used for all CO_2 detection experiments, whereas CF_4 was used for CO detection. The slow rise component of the CO transient signal is attributed to the rather slow relaxation of vibrationally excited CO. For HCNO, no literature information is available regarding vibrational relaxation rates. Figure 2 shows HCNO transient signals obtained at different SF_6 pressures. The rise time of the transients decreases with increasing SF_6 pressure, as is expected if SF_6 is an effective vibrational relaxer. As a result, we used SF_6 buffer gas for HCNO detection experiments, and we are confident that the rovibrational populations of all of the probed molecules are

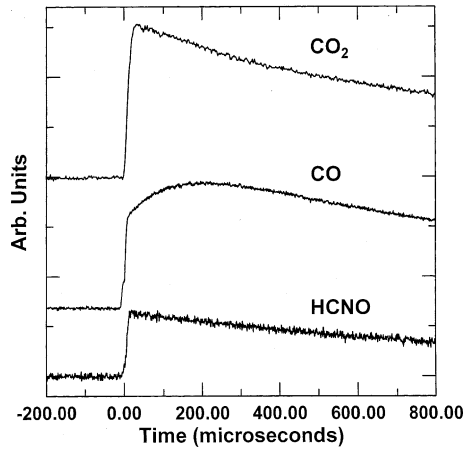

Figure 1. Transient infrared absorption signals for CO, HCNO, and CO_2 product molecules. Reaction conditions: $P_{C_2H_5OCCH} = 0.01$ Torr, $P_{NO} = 0.6$ Torr, $P_{Xe} = 1.0$ Torr, $P_{SF_6} = 1.0$ Torr (CO_2 and HCNO signals), $P_{CF_4} = 1.0$ Torr (CO signals only).

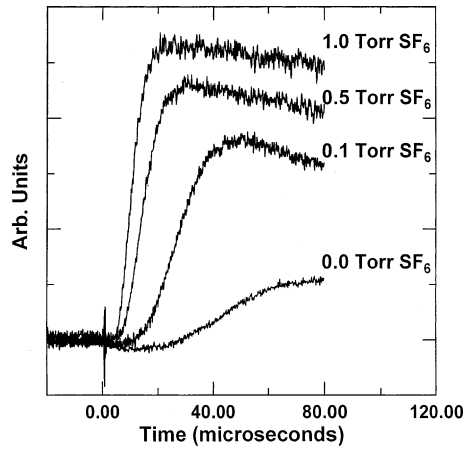

Figure 2. Transient infrared absorption signals for HCNO product molecules as a function of SF_6 buffer gas pressure. Reaction conditions: $P_{C_2H_5OCCH} = 0.01$ Torr, $P_{NO} = 0.3$ Torr, $P_{SF_6} = 0.0-1.0$ Torr.

relaxed to a Boltzmann distribution within ~150 μs. The slow ~1 ms decay present in all of the transient signals is attributed to diffusion of product molecules out of the probed region of the reaction cell.

Attempts to detect N_2O product molecules in this reaction system were unsuccessful. If channel (1c) is active, one expects N_2O formation in high yield via the secondary reaction:

$$NCO + NO \rightarrow N_2O + CO \quad (2a)$$

$$\rightarrow CO_2 + N_2 \quad (2b)$$

Previous experiments have shown that $\phi_{2a} = 0.44$ at 298 K.[25] Our failure to detect N_2O indicates that channel (1c) does not contribute significantly to the title reaction. This is a more sensitive test for channel (1c) than direct NCO detection by infrared spectroscopy[37] because N_2O has much greater infrared linestrengths. In addition, N_2O formation could also originate from reactions of CH radicals formed by photolysis of HCCO radicals:

$$C_2H_5OCCH + h\nu\ (193\ nm) \rightarrow C_2H_5 + HCCO$$

$$HCCO + h\nu\ (193\ nm) \rightarrow CH + CO$$

$$CH + NO \rightarrow HCN + O$$

$$\rightarrow NCO + H$$

$$\rightarrow NH + CO$$

$$NCO + NO \rightarrow N_2O + CO$$

$$\rightarrow CO_2 + N_2$$

Our failure to detect N_2O therefore also indicates that these multiple photon effects are not significant in this experiment, and that significant quantities of CH radicals are not formed. This is an important point, because the presence of CH would substantially complicate the secondary chemistry in these experiments.

Some transient signals were collected with the inclusion of Xe buffer gas in addition to the CF_4 or SF_6 buffer gas. This experiment was to test for effects due to possible excited electronic states of HCCO, which are likely to be relaxed by xenon. The transient signals were identical with and without xenon, suggesting that excited electronic states do not affect our results.

Absorption signals for CO, CO_2, and N_2O products were converted to number densities using tabulated line strengths[30] and equations described previously.[26] For HCNO, no literature information on infrared line strengths is available. Instead, we calibrated HCNO signals by directly measuring the static infrared absorption of authentic samples of HCNO synthesized in our laboratory. Figure 3 shows a plot of this calibration. This measurement was somewhat complicated by the tendency of HCNO to quickly decompose, especially when in contact with metal (stainless steel) vacuum lines. To minimize decomposition, the HCNO sample was kept frozen except when needed to fill the absorption cell. The static absorption signal was measured within approximately ~0.5 min of filling of the cell, and contact with metal was minimized. Each point in Figure 3 represents a new fill of the absorption cell.

An important test for background sources of the detected molecules is to check whether the transient signals are observed in the absence of nitric oxide reagent, i.e., upon photolysis of a C_2H_5OCCH/buffer gas mixture. We find negligible amounts of CO_2 and HCNO formation under these conditions, but

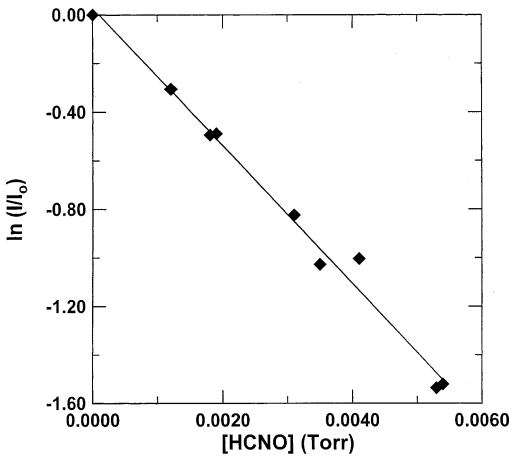

Figure 3. Beers law plot of the calibration of HCNO static infrared absorption signal, using the R(10) line at 2203.851 cm^{-1}.

significant amounts of CO are observed (approximately one-third to one-half of the CO signal when NO reagent is included in the reaction mixture). This background CO could originate from several sources: it is possible that C_2H_5OCCH has a minor photolysis channel for CO formation, although no such channel was reported in the photolysis study of this precursor.[24] In the absence of NO reagent, photolytically produced HCCO may react with trace amounts of oxygen impurities, HCCO may react with C_2H_5OCCH, or HCCO may react with itself (or other radicals), producing some CO. It is also possible that multiple photon effects (such as HCCO photolysis) may contribute to the CO formation. We note that similar (although smaller) CO background signals were observed in a recent study of the HCCO + O_2 reaction.[25] It is not clear which of these sources of background CO are most important. An excimer laser power dependence study showed only a slight nonlinearity in the CO yield vs excimer pulse energy, suggesting that multiple photon effects are minor. The lack of observed N_2O production described above supports this conclusion. In principle, some of these background sources (such as radical−radical chemistry or trace O_2 reactions) should result in a longer rise time than would be expected from CO originating from the title reaction. Unfortunately, our CO absorption signals (see Figure 1) always display a long rise time component because the relaxation of vibrationally excited CO (mainly by CF_4 buffer gas) is quite slow. Our experimental result is that the CO transient collected in the absence of NO reagent has a slighly longer rise time in the slow rise component than that collected with NO reagent, but the difference is insufficient to allow us to effectively discriminate against the background. We suspect that reactions of HCCO (with itself, precursor, trace O_2, etc.) are responsible for most of the background. If this is true, such reactions are virtually entirely suppressed when excess NO reagent is included, and therefore this background signal should not be subtracted from the signal with NO. Under this assumption, the CO and CO_2 signals upon photolysis of a C_2H_5OCCH/NO/buffer gas mixture are predominantly due to the title reactions, with little or no contribution from secondary chemistry. The relative yields of these two products is therefore a direct measurement of the branching ratio. Using this approach, we determine $\phi_{1a} = 0.23 \pm 0.03$ and $\phi_{1b} = 0.77 \pm 0.03$.

An alternative approach to determining the branching ratio of the title reaction is to compare the HCNO and CO_2 yields. This avoids the uncertainties inherent in the above discussion of background sources of CO. The key here is that unlike most previous literature on the HCCO + NO reaction, our HCCO

TABLE 1: Product Branching Ratio of the HCCO + NO Reaction[a]

CO_2 + HCN	HCNO + CO	method	ref
0.81	0.19	ab initio	13
0.23 ± 0.09	0.77 ± 0.09	DF/MS (700 K)	6
0.65	0.35	modeling (1100 K)	14
0.28 ± 0.10	0.64 ± 0.12	FP/FTIR	18
0.12 ± 0.04	0.88 ± 0.04	FP/IR	19
0.22	0.78	ab initio	20
0.27	0.73	ab initio	21
0.22 ± 0.04	0.78 ± 0.04	FP/IR	this work

[a] All values at 296 K unless otherwise indicated. Abbreviations: DF/MS = discharge flow/mass spectrometry. FP/IR = flash photolysis/infrared absorption.

formation method does not produce CH_2 radicals, and therefore the $CH_2 + NO \rightarrow HCNO + H$ secondary reaction does not contribute to the HCNO yield. Comparison of HCNO and CO_2 yields is therefore a direct measurement of the branching ratio. The disadvantage of this approach is the requirement to calibrate the HCNO signals, as described above. Using this method, we obtain $\phi_{1a} = 0.21 \pm 0.04$ and $\phi_{1b} = 0.79 \pm 0.04$, nearly identical to the value obtained using CO. In other words, our calibration of the HCNO signals yields HCNO yields very similar to the CO yields obtained, as is expected if secondary chemistry does not significantly affect the yields of these molecules.

On the basis of both sets of data, we recommend the value $\phi_{1a} = 0.22 \pm 0.04$ and $\phi_{1b} = 0.78 \pm 0.04$ for the branching ratio at 296 K. Table 1 shows this and other literature values for the branching ratio. Our value is in good agreement with the two most recent computational studies of this reaction, which predict $\phi_{1a} = 0.22$[20] and $\phi_{1a} = 0.27$[21] at 296 K. Our experiments suggest the ab initio studies are sufficiently accurate to reliably predict the branching ratios at high temperature. Our results are somewhat different than those of our earlier study using ketene precursor,[19] but are in reasonable agreement with the FTIR study of Eickhoff and Temps,[18] In addition, our results are virtually identical to the values obtained by Boullart et al. at 700 K,[6] indicating that the branching ratio is virtually independent of temperature over the range 300−700 K. This is also in agreement with the ab initio calculations, which predict only a very slight decrease in ϕ_{1a} with increasing temperature.

Conclusions

The HCCO + NO reaction has been studied using a new precursor for HCCO formation. Detection of CO, CO_2, and HCNO product yields the following branching ratio at 296 K: $\phi_{1a} = 0.22 \pm 0.04$ and $\phi_{1b} = 0.78 \pm 0.04$. These values are in good agreement with other recent experimental and computational studies.

Acknowledgment. This work was supported by the Division of Chemical Sciences, Office of Basic Energy Sciences of the Department of Energy, Grant DE-FG03-96ER14645.

References and Notes

(1) Brock, L. R.; Mischler, B.; Rohlfing, E. A.; Bise, R. T.; Neumark, D. M. *J. Chem. Phys.* **1997**, *107*, 665.
(2) Brock, L. R.; Mischler, B.; Rohlfing, E. A. *J. Chem. Phys.* **1999**, *110*, 6773.
(3) Osborn, D. L.; Mordaunt, D. H.; Choi, H.; Bise, R. T.; Neumark, D. M.; Rohlfing, C. M. *J. Chem. Phys.* **1996**, *106*, 10087.
(4) Unfried, K. G.; Glass, G. P., Curl, R. F. *Chem. Phys. Lett.* **1991**, *177*, 33.
(5) Temps, F.; Wagner, H. Gg.; Wolf, M. *Z. Phys. Chem.* **1992**, *176*, 27.
(6) Boullart, W.; Ngugen, M. T.; Peeters, J. *J. Phys. Chem.* **1994**, *98*, 8036.
(7) Nguyen, M. T.; Boullart, W.; Peeters, J. *J. Phys. Chem.* **1994**, *98*, 8030.
(8) Peeters, J.; Boullart, W.; Devriendt, K. *J. Phys. Chem.* **1995**, *99*, 3583.
(9) Carl, S. A.; Sun, Q.; Vereecken, L.; Peeters, J. *J. Phys. Chem. A* **2002**, *106*, 12242.
(10) Vinckier, C.; Schaekers, M.; Peeters, J. *J. Phys. Chem.* **1985**, *89*, 508.
(11) Schmoltner, P. M.; Chu, P. M.; Lee, Y. T. *J. Chem. Phys.* **1989**, *91*, 5365.
(12) Chen, S. L.; McCarthy, J. M.; Clark, W. D.; Heap, M. P.; Seeker, W. R.; Pershing, D. W. *Symp. (Int.) Combust Proc.* **1986**, *21*, 1159.
(13) Miller, J. A.; Durant, J. L.; Glarborg, P. *Symp. (Int.) Combust. Proc.* **1998**, *27*, 235.
(14) Glarborg, P.; Alzueta, M. U.; Dam-Johansen, K.; Miller, J. A. *Combust. Flame* **1998**, *115*, 1.
(15) Miller, J. A.; Bowman, C. T. *Prog. Energy Combust. Sci.* **1989**, *15*, 287.
(16) Prada, L.; Miller, J. A. *Combust. Sci. Technol.* **1998**, *132*, 225.
(17) Miller, J. A.; Klippenstein, S. J.; Glarborg, P. *Combust. Flame* **2003**, *135*, 357.
(18) Eickhoff, U.; Temps, F. *Phys. Chem. Chem. Phys.* **1999**, *1*, 243.
(19) Rim, K. T.; Hershberger, J. F. *J. Phys. Chem. A* **2000**, *104*, 293.
(20) Vereecken, L.; Sumathy, R.; Carl, S. A.; Peeters, J. *Chem. Phys. Lett.* **2001**, *344*, 400.
(21) Tokmakov, I. V.; Moskaleva, L. V.; Paschenko, D. V.; Lin, M. C. *J. Phys. Chem. A* **2003**, *107*, 1066.
(22) Glass, G. P.; Kumaran, S. S.; Michael, J. V. *J. Phys. Chem. A* **2000**, *104*, 8360.
(23) Eshchenko, G.; Koecher, T.; Kerst, C.; Temps, F. *Chem. Phys. Lett.* **2002**, *356*, 181.
(24) Krisch, M. J.; Miller, J. L.; Butler, L. J.; Su, H.; Bersohn, R.; Shu, J. *J. Chem. Phys.* **2003**, *119*, 176.
(25) Osborn, D. L. *J. Phys. Chem. A* **2003**, *107*, 3728.
(26) Cooper, W. F.; Park, J.; Hershberger, J. F. *J. Phys. Chem.* **1993**, *97*, 3283.
(27) Rim, K. T.; Hershberger, J. F. *J. Phys. Chem. A* **1998**, *102*, 5898.
(28) Pasinszki, T.; Kishimoto, N.; Ohno, K. *J. Phys. Chem. A* **1999**, *103*, 6746.
(29) Wentrup, C.; Berecht, B.; Briehl, H. *Angew. Chem., Int. Ed. Engl.* **1979**, *18*, 467.
(30) Rothman, L. S.; et al. *J. Quant. Spectrosc. Radiat. Transfer* **1992**, *48*, 469.
(31) Ferretti, E. L.; Rao, K. N. *J. Mol. Spectrosc.* **1974**, *51*, 97.
(32) Cooper, W. F.; Hershberger, J. F. *J. Phys. Chem.* **1992**, *96*, 771.
(33) Fakhr, A.; Bates, R. D. Jr. *Chem. Phys. Lett.* **1980**, *71*, 381.
(34) Stephenson, J. C.; Moore, C. B. *J. Chem. Phys.* **1970**, *52*, 2333.
(35) Richman, D. C.; Millikan, R. C. *J. Chem. Phys.* **1975**, *63*, 2242.
(36) Green, W. H.; Hancock, J. K. *J. Chem. Phys.* **1973**, *59*, 4326.
(37) Brueggemann, R.; Petri, M.; Fischer, H.; Mauer, D.; Reinert, D.; Urban, W. *Appl. Phys. B* **1989**, *48*, 105.